Optica Applicata, Vol. XLV, No. 3, 2015
DOI: 10.5277/oa150307

Design and analysis of low bend losses of the air core optical fiber for wavelength selective devices

VIKRAM PALODIYA, SANJEEV KUMAR RAGHUWANSHI*

Department of Electronics Engineering, Indian School of Mines, Dhanbad-826004, Jharkhand, India

*Corresponding author: sanjeevrus@yahoo.com

In this paper, the bending loss, modal field diameter and the modal field distribution of the air core optical fiber are investigated. The effect of optical and geometrical parameters on the bending loss, power confinement and modal field diameter are examined in this special fiber. Detailed design parameters and operation principles of the air core optical fiber are discussed. The structure is based on a unique three layered structure of air core optical fiber, having the central air core, germanium silicate ring core, and silica cladding. It has been demonstrated that air core optical fiber has an excellent mode transformation capability. The air core optical fiber is expected to have a versatile application in local area optical communication networks and tunable wavelength selective devices. The main advantages of air core optical fiber are low bend loss and small mode field diameter, which is a prime focus of this paper.

Keywords: air core optical fiber, bending loss, mode field distribution, optical mode converter.

1. Introduction

For the last three decades, there is a tremendous development of optical fiber technology for optical communications in order to increase transmission distance, data rate and bandwidth. The conventional optical fiber consists of a solid glass core with a higher refractive index circumscribed by cladding with a relatively lower refractive index. There are three major transmission optical fibers: single-mode fibers (SMFs), dispersion compensating fibers (DCFs) and non-zero dispersion shifted fibers (NZDSFs). Due to the replacement of telephonic wire with optical fiber worldwide in the end of the 20th century, the demand for silica based special fibers has increased manifold. Hence, the dispersion shifted fiber (DSF) magnificently developed and deployed to obtain larger communication capacity by optimization of the chromatic dispersion on the *S*-, *C*-, and *L*-bands. Alongside with these transmission fibers, especially fibers such as rare earth-doped fibers, attenuation fibers, photosensitive fibers, and polarization maintaining fibers have been also developed for optical devices.

These fibers, however, do have the common platform as transmission fibers in a sense that they do share the solid glass core/cladding structures. Recently, there have been new technical challenges to develop fibers with an air core to provide optical functions and improve characteristics that were not available in conventional solid core fibers. Holey fibers [1], omni-guide fibers [2], hollow IR transmitting fibers [3], and hollow core optical fibers [4] have been recently introduced to unusual guiding structures and subsequently demonstrated varieties of new passages of novel applications. These holey air silica structured optical fibers have been intensively examined for their unique and extraordinary optical properties, such as continuous single mode operation [5] and unusual group-velocity dispersion (GVD) in the visible region [6] utilizing a very powerful new degree of freedom in fiber design, the period of air core. In most conventional fiber devices the wave guidance is achieved by the total internal reflection in the effective step index guiding structure where the index near the central part is raised by silica defects keeping the effective index in the cladding lower. However in a photonic crystal fiber or holey fiber, the light guidance takes place by diffraction phenomena rather than reflection phenomena. Recently, defects in this guiding air core optical fiber (ACOF) have also opened a new way of producing a low mode field diameter and bend loss by changing core diameter. Utilizing these features, varieties of recent fiber devices have been proposed to control optical power, polarization and spectral response [7–9]. Omni-guide fibers are based on the radial periodic structure of high and low index concentric rings, which is provided by high refractive index glasses and low refractive index polymer. In contrast, ACOFs have a central air core, where the majority of optical power is carried axially by the radial photonic Bragg condition. Similarly, hollow IR transmitting hollow fibers carry the optical fiber through the central air hole by reflective metal or metal-insulator coating on the inner surface of the holey fiber. These types of fibers can be applied in practice as mode convertors or optical filters, to mention just a few devices.

2. Theory of air core optical fiber (ACOF)

A step depressed core optical fiber consists of an inner air core surrounding the raised index germanium silicate ring core and a silica cladding as shown in Fig. 1. The numerical analysis of ACOF should be done by a full vectorial calculation. We design a low bend fiber to achieve the large index difference between the inner air core and the outer ring core. However, as far as a mode cut-off was concerned, the linearly-polarized, the weakly guiding approximation is still valid. To confirm this, the results using the LP mode assumption and commercial software (Opti-fiber) that uses a full vectorial simulation were compared. The error in the calculated effective indices of modes was within 1% in most cases.

Due to the reason mention above, the weakly guiding approximation and the linearly polarized LP modes were considered for simplicity. This assumption will also be applied to the numerical approach to the properties of the ACOF, which will be further discussed. The refractive indices of the ring core, cladding and the air core sections

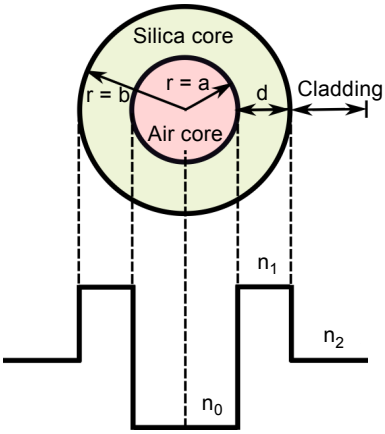

Fig. 1. Cross-sectional view and refractive index profile of an air core optical fiber.

are n_{core}, n_{clad} (= 1.647 or 1.450) and n_{air} (= 1), respectively. The air core, ring core and cladding radii are r_{air}, r_{core} and r_{clad}, respectively. Here, the core thickness T is defined as

$$T = r_{\text{core}} - r_{\text{air}} \tag{1}$$

The electric field component of guided modes is defined as

$$E(r, \varphi, z) = e(r)\exp(-j\varphi l)\exp(-j\beta z), \qquad l = 0, \pm 1, \pm 2, \ldots \tag{2}$$

where r, φ are the radial and tangential co-ordinates in the plane perpendicular to the fiber axis and z is the length axis of the fiber. Here $e(r)$ is an solution of the Helmholtz equation, which means the radial dependence of the electric field component. It can be written as follows [10]:

$$e(r) = \begin{cases} AI_l(vr) & r < r_{\text{air}} \\ BJ_l(ur) + CY_l(ur) & r_{\text{air}} \le r \le r_{\text{core}} \\ DK_l(wr) & r > r_{\text{core}} \end{cases} \tag{3}$$

Here, r is the radial position and A, B, C and D are constants where I_l (K_l) is the l-th order modified Bessel function of the first (second) kind and J_l (Y_l) is the l-th order Bessel function of the first (second) kind; v, u and w are the model parameters and they are defined as

$$v = \sqrt{\beta^2 - n_{\text{air}}^2 k_0^2} \tag{4}$$

$$u = \sqrt{n_{\text{core}}^2 k_0^2 - \beta^2} \tag{5}$$

$$w = \sqrt{\beta^2 - n_{\text{clad}}^2 k_0^2} \tag{6}$$

Here, the eigenvalue β is the propagation constant of each mode and k_0 is the wave number. By applying the continuity of electric field at two boundaries $r = r_{\text{air}}$ and r_{core}, the following 4×4 matrix type characteristic equation can be obtained [11]:

$$\begin{vmatrix} I_l(vr_{\text{air}}) & -J_l(ur_{\text{air}}) & -Y_l(ur_{\text{air}}) & 0 \\ vI_l'(vr_{\text{air}}) & -uJ_l'(ur_{\text{air}}) & -uY_l'(ur_{\text{air}}) & 0 \\ 0 & J_l(ur_{\text{core}}) & -Y_l(ur_{\text{core}}) & -K_l(wr_{\text{core}}) \\ 0 & uJ_l'(ur_{\text{core}}) & -uY_l'(ur_{\text{core}}) & -wK_l'(wr_{\text{core}}) \end{vmatrix} = 0 \quad (7)$$

The propagation constant β can be obtained from Eq. (7) numerically and for each azimuthal index l, the characteristic equation has multiple solutions yielding discrete propagation constants β_{lm} (m = 1, 2, ...), which represents a guided mode. The transverse field distribution of each mode can be computed from Eq. (3) after determining the constants A, B, C and D from the achieved propagation constant (β) value. A primary target of the ACOF is a distributed fiber waveguide filter for high power fiber laser sources operating at short wavelengths. Therefore, calculating fiber parameters for the fundamental mode cut-off is the main objective here in this paper. In order to obtain the fundamental mode cut-off wavelength, the propagation constant of the LP_{01} mode at several core thicknesses was calculated depending on wavelength and then it was converted to the effective index, which is defined as $n_{\text{eff}} = \beta/k_0$. Figure 2 shows the variation of the effective indices of the LP_{01} mode depending on core thickness and wavelength at a fixed core diameter of 6 μm. Here, the maximum powers transfer through the ring core and the minimum powers transfer through the central air core.

In general, the modal cut-off wavelength takes place when the effective index of the guided mode becomes equal to the silica cladding index. After cut-off wavelength, the mode does not guide through the core any more. However, it is found while doing simulation that ACOF shows a fundamental LP_{01} mode cut-off wavelength. In case of ACOF, the mode cut-off occurs when the effective index n_{eff} of the LP_{01} mode becomes equal to the silica cladding index n_{clad}. Beyond this wavelength, the fundamental mode does not exist in the core. This property is similar to that of a W-type fiber, which exhibits the waveguide filter characteristics [12]. The appearance of the fundamental mode cut-off in an ACOF is due to the negative value of the volume integration of a relative refractive index in a hollow structure (because of its central air core section) [13]. For the case of ACOF, the effective index and cut-off wavelength of few lower order modes are shown in Table 1.

In the ACOF, the air core has an effect on mode characteristics too as it is apparent from Table 1. In Table 1, the effective index and cut-off wavelength were calculated at a fixed core radius of 3 μm. Here, the refractive index of silica cladding was assumed

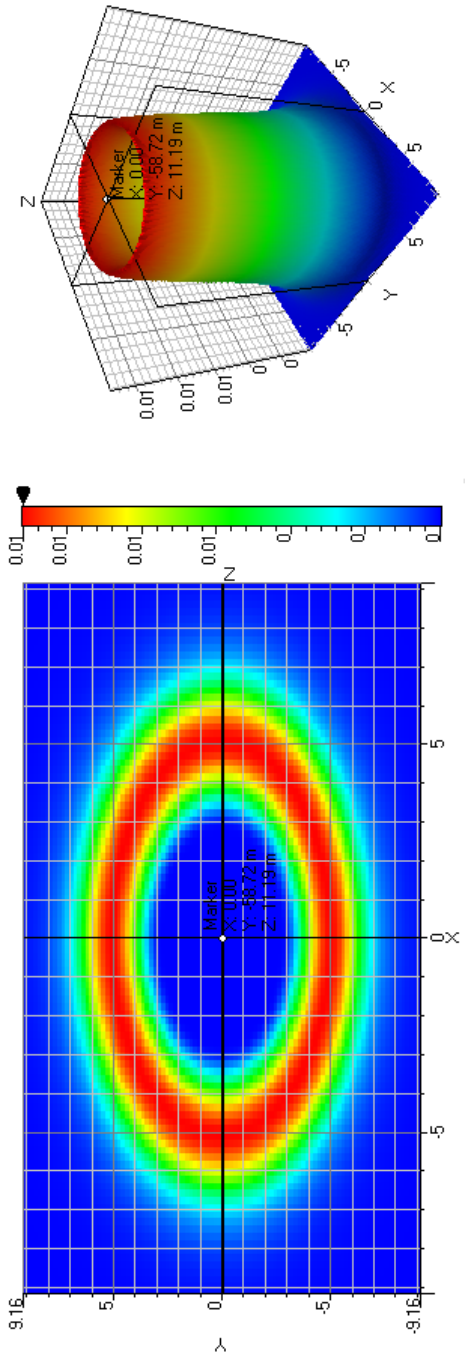

Fig. 2. The top view of fundamental LP_{01} mode (**a**) and three-dimensional view of LP_{01} mode (**b**).

T a b l e 1. Air core optical fiber parameters for different modes.

Mode	Effective index	Cut-off wavelength [μm]
LP_{01}	1.6404278	No cut-off wavelength
LP_{11}	1.6397929	2.4205151
LP_{21}	1.6379477	1.8916550
LP_{31}	1.6351027	1.5099087

to be 1.45, which indicates that the dependence on the air core width in the cut-off wavelength of the LP_{01} mode is small. However, the effective indices of the LP_{01} mode at shorter wavelengths were different, depending on the core width, which in fact will affect the properties of ACOF. For example, the low effective index of LP_{01} at a given wavelength could be detrimental to the bending performances of the LP_{01} mode in the fiber. In terms of the fiber waveguide filter, the bending loss is highly related to the sharpness of the filter. For the higher order mode LP_{11}, the cut-off wavelength has shifted to the longer wavelength side while the core width is increased. In the case of ACOF with the core radius of 3 μm, the effective index of the LP_{11} mode significantly closes to that of the LP_{01} mode, which means that the fiber with the larger core width can easily be multi-mode and it is difficult to separate the higher order modes from the fundamental (LP_{01}) mode. Therefore, for the gain medium, if the core width becomes wide, the core area can be relatively increased and this improves the pump absorption in a cladding pump configuration, while the single-mode operation at a desired wavelength will become more challenging.

3. Computation of modal field distribution in air core optical fiber (ACOF)

The propagation constants β and the parameters v, u and w are calculated from the characteristic Eq. (7). Also, by applying the boundary conditions (field continuity at $r = r_{air}$ and r_{clad}), the constants A, B, C and D can be calculated numerically from Eq. (3). After obtaining all these parameters, the modal field distribution of LP modes supported by the ring-core can be obtained. Figure 3 shows the modal field distributions of different modes (LP_{01}, LP_{11}, LP_{21} and LP_{31}) in an ACOF with a 3 μm air core radius and a 3.5 μm outer core thickness. In order to see another higher order mode, the core index was increased while the wavelength was considered to be 1.550 μm. The modal field distribution of the LP_{01} mode was doughnut in shape and the optical field is well confined in the ring core. However, the field component in the central air region is very weak, while it is relatively strong in the ring core and the field is broadened from the ring-core to the silica cladding, which causes the increase of the mode field diameter. Hence we consider the smaller core radius throughout because the core radius controlled the effective mode field diameter. The higher order mode fields are also formed in the ring core, whose cut-off characteristics are significantly dependent on the air core width. The cut-off wavelength of higher order modes (LP_{11}, LP_{21} and LP_{31}) are 2.421, 1.892 and 1.510 μm, respectively, as it is revealed in Table 1 too. For a fiber laser, the mode confinement factor (overlap factor with a doped core) of the signal is one of important parameters, because the signal gain linearly increases depending on the mode confinement factor [14, 15]. Figure 3 shows the modal field distribution of ACOF at wavelength 1.55 μm for few modes cases.

When the effective index n_{eff} is close to the refractive index n_{clad} of the silica cladding, the modal parameter u is increasing and w decreases, and the field penetrates

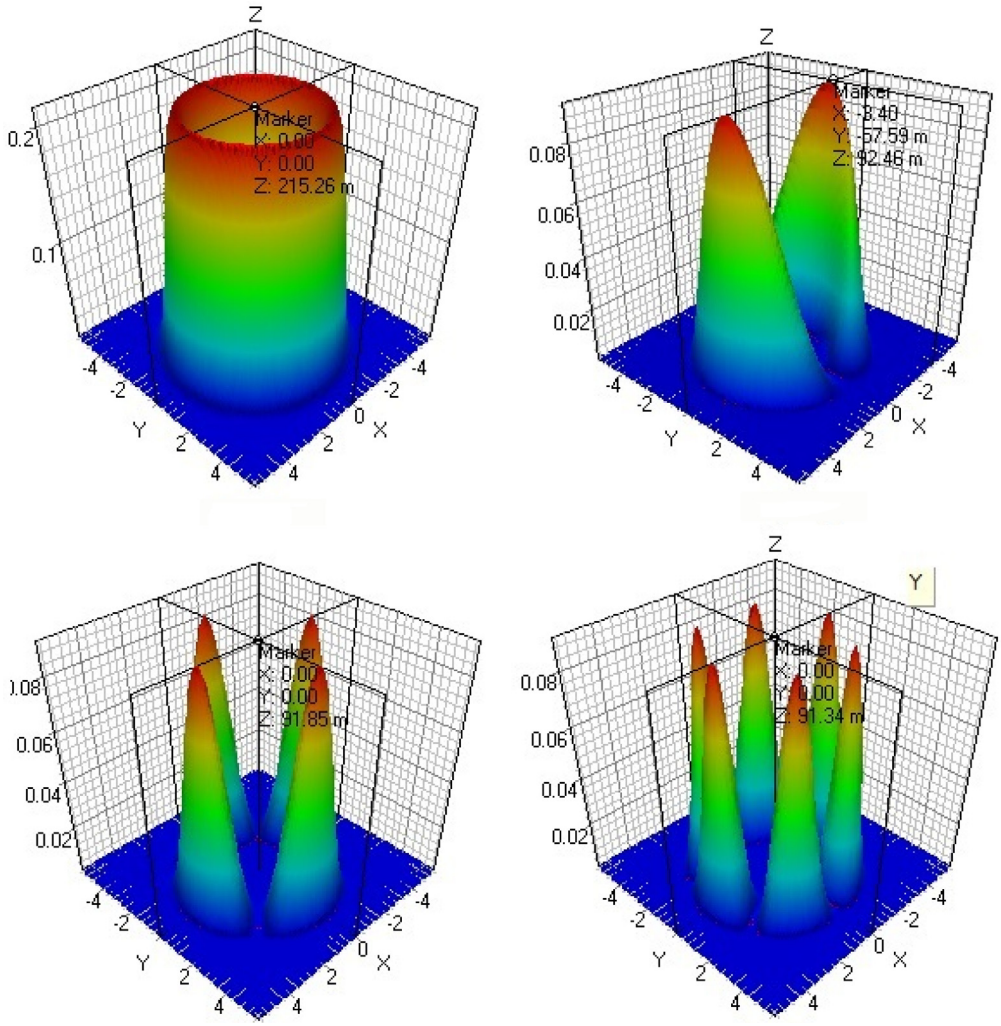

Fig. 3. Modal field distribution of ACOF at wavelength 1.55 µm (inner core radius: 3 µm, outer core thickness: 3.5 µm), LP_{01} (**a**), LP_{11} (**b**), LP_{21} (**c**), and LP_{31} (**d**).

deeper into the silica cladding. Figure 4 shows the normalized power confinement distribution along the radial distance which was calculated at specific core thicknesses. Figure 4 reveals that although the centre core is composed of air, the majority of energy is confined in the surrounding high-index ring; therefore, the ACOF is different from the air-core bandgap fiber which is guiding light in the air core. Considering the smaller core area and the deformed mode field, such fiber seems to have specific applications in optical communication. It has been found during simulation that as the wavelength of the light approaches towards the fundamental mode cut-off wavelength of the fiber, the modal confinement factor is significantly reduced and the field gets broader.

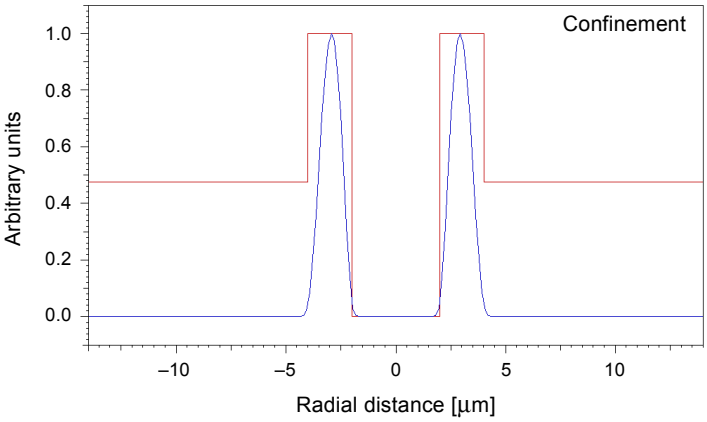

Fig. 4. Variation of power confinement with the radial distance at wavelength 1.55 μm.

Beyond the fundamental mode cut-off, where $n_{\text{eff}} = n_{\text{clad}}$, the modal field does not exist in the ring core any more. This makes the ACOF suitable for a distributed wavelength filter.

4. Mode field diameter (MFD) in air core optical fiber (ACOF)

The MFD is an important parameter related to the optical field distribution in the fiber. It has been shown that MFD provides useful information about the cabling performances, such as possible joint, macro-bending, and micro-bending losses. In an optical signal, not all the light travels through the core of the fiber. The optical power is distributed between the core and the cladding. The mode field represents the distribution of light through the core and cladding of a particular fiber. The near-field mode field diameter (n-MFD) is defined as: it is the diameter at which the near-field power falls to $1/e^2$ of its maximum value [16]. Hence it can be written as

$$d_n = 2\sqrt{2}\left(\frac{\int_0^\infty E^2(r)\, r^3 \,\mathrm{d}r}{\int_0^\infty E^2(r)\, r \,\mathrm{d}r}\right)^{1/2} \tag{8}$$

where $E(r)$ is the optical mode field distribution. The far-field mode field diameter (f-MFD) is defined as: it is the diameter at which the far-field power falls to $1/e^2$ of its maximum value. It can be written as

$$d_f = 2\sqrt{2}\left(\frac{\int_0^\infty E^2(r) r \,\mathrm{d}r}{\int_0^\infty [E'(r)]^2 r \,\mathrm{d}r}\right)^{1/2} \tag{9}$$

Finally the effective mode field diameter (eff-MFD) is written as

$$d_{\text{eff}} = 2\sqrt{2}\,\frac{\int E_i^4 r\,\mathrm{d}r}{\left[\int E_i^4 r\,\mathrm{d}r\right]^{1/2}} = \frac{2}{\pi}\sqrt{A_{\text{eff}}} \tag{10}$$

where A_{eff} is the effective mode area.

5. Calculation of bending loss of air core optical fiber (ACOF)

Bending loss in the fiber is one of important issues of high power fiber laser sources. A high bending loss at the signal wavelength degrades the amplifier performance by reducing the gain. In addition, for compact devices, a bend-resistant fiber may be needed. In a cladding-pumped configuration, the signal that escapes from the core caused by bending can become a noise source which may cause cladding mode lasing or amplified stimulated emission (ASE) noise due to mode-mixing or mode-coupling between the fundamental mode and other higher modes. In order to study the bending loss property of ACOF, the uniform bending loss α_{bending} formula for an arbitrary index profile single mode fiber derived from SAKAI and KIMURA [17] is used

$$\alpha_{\text{bending}} = \frac{\sqrt{\pi}\,A_{cl}^2 \exp\left(-\dfrac{\sqrt{2}}{3}\,\dfrac{\lambda^2 R}{\pi^2 n_{\text{core}}^2 W_\infty^3}\right)}{2P_t\left(\dfrac{\sqrt{2}}{W_\infty}\right)^{3/2}\left(R + \dfrac{2\pi^2 n_{\text{core}}^2 W_\infty^2 r_{\text{core}}}{\lambda^2}\right)^{1/2}} \tag{11}$$

where R is the bending radius, n_{core} is the refractive index of the core, r_{core} is the core radius, λ is the operating wavelength. Here W_∞ is the new mode field radius representing the bend sensitivity. This is defined by the propagation constant β of the LP_{01} mode and the wave number in the cladding k_{clad} as follows [18]:

$$W_\infty^2 = \frac{2}{\beta^2 - k_{\text{clad}}^2} \tag{12}$$

The bend sensitivity is determined by the propagation constant β, which is varied by the core width, the refractive index difference between the core and cladding, and the wavelength. When β approaches the wave number in the cladding k_{clad}, the bend sensitivity is significantly increased. It means that the index difference between the effective core index n_{eff} and silica cladding is related to the bending loss. The smaller it is, the higher the bending loss becomes [19, 20]. In Eq. (11), A_{cl}^2/P_t is another important parameter, which represents the normalized field intensity coefficient in the cladding region. This parameter can be obtained from the following relations:

$$e(r) = A_{cl} k_0\left(\frac{\sqrt{2}}{W_\infty} r\right), \qquad r > r_{\text{core}} \tag{13}$$

$$P_t = \int_0^\infty e^2(r) r \, \mathrm{d}r \tag{14}$$

where $e(r)$ is the radial field function in the cladding, A_{cl} is the coefficient of the field function, and k_0 is the modified Bessel function of the first order. Here P_t is the integrated field intensity, which is determined by the radial field distribution $e(r)$ in the cladding. For the distributed wavelength waveguide filter, the bend sensitivity is very high around the fundamental mode cut-off wavelength range, because the effective index n_{eff} of the fundamental mode is close to the refractive index of the silica cladding n_{clad}. In the case of an ACOF, the bending loss is significantly increased just before reaching the fundamental mode cut-off wavelength. The bending loss is maintained at a low value far from the fundamental mode cut-off wavelength to the shorter wavelength side. Although the fundamental mode cut-off in the ACOF is well-defined in theory ($n_{\text{eff}} = n_{\text{clad}}$), the mode cut-off wavelength is difficult to define in a real case because of the very high bend-sensitivity near the theoretical fundamental mode cut-off wavelength.

The bending loss and effective indices as a function of the wavelength were calculated in the ACOF at several bending radii using Eqs. (11)–(14). The theoretical fundamental mode cut-off wavelength was 1.53 μm. At this wavelength, the bending loss of the LP_{01} mode is significantly higher, which indicates that the light cannot be confined any more in the ring-core. Further coiling causes a huge bending loss on the shorter wavelength side and it effectively makes the fundamental mode cut-off wavelength shift to shorter wavelengths. In practice, the induced 70% loss of the power per unit length is large enough for the fiber to be considered as "non-guiding". Based

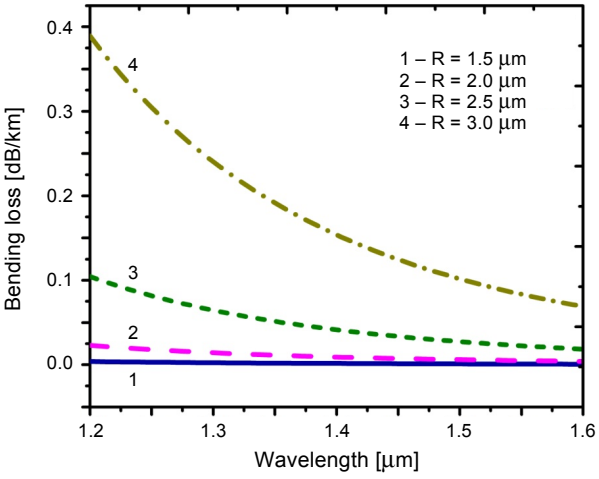

Fig. 5. Bending loss *versus* wavelength for different core radius depends on wavelength.

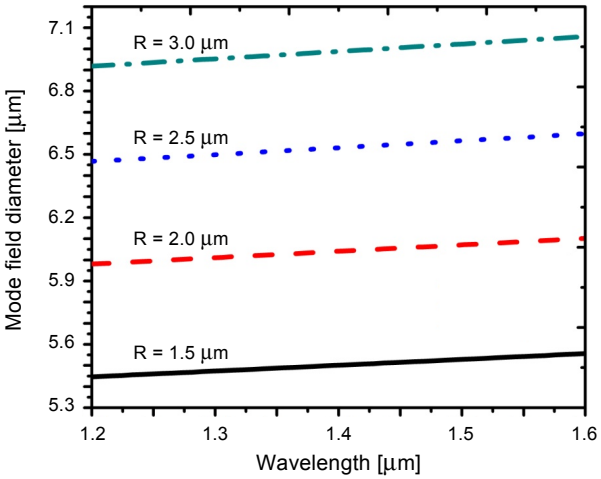

Fig. 6. Mode field diameter *versus* wavelength for different core radius.

on this, the fundamental mode cut-off wavelength can be defined practically, which is called as the effective fundamental mode cut-off wavelength. Figure 5 presents the effect of the core radius R on the bending loss. It can be seen that the bending loss decreases when R decreases. Also it is useful to mention that at constant value of R, the bending loss decreases with an increase in the wavelength. The ACOF gives the good result at R equal to 3 µm. It should be noted that a smaller core further gives a smaller effective core area and the deformed mode field.

Figure 6 reveals the change in MFD as a function of wavelength at different core radius. It is apparent from Fig. 6 that as the core radius and wavelength increase, MFD also increases. Since the mode field is mainly confined in the high-index layer, and as the core radius increase, the area of the high-index layer is also increased. Therefore, the MFD should depend on the area of the high-index layer.

6. Conclusion

We have investigated a new structure along with an expanded degree of freedom in design and manipulation of optical characteristics in an air core optical fiber. We have analysed mode field distribution in different modes, bend losses, mode field diameter and power confinement in a ring core. The simulation results show the effect of the core radius on modal field diameter, the bending losses and mode field diameter. It is more beneficial for an optical communication point of view. This design is applicable in an all-fiber tunable wavelength selective device based on ACOF-like mode converter and waveguide filters. This design and information are useful for low bending loss transmission optical communication networks.

Acknowledgements – The authors would like to thank the Ministry of Human Resource Development (MHRD), Government of India, New Delhi and Indian School of Mines Dhanbad for the financial support

to provide the Opti-Fiber Software to carry out this research work. Dr. Sanjeev Kumar Raghuwanshi wishes to thank to the Director of Indian School of Mines, Dhanbad, India for constant encouragement during this research work.

References

[1] KNIGHT J.C., RUSSELL P.S.J., *New ways to guide light*, Science **296**(5566), 2002, pp. 276–277.

[2] FINK Y., RIPIN D.J., SHANHUI FAN, CHIPING CHEN, JOANNEPOULOS J.D., THOMAS E.L., *Guiding optical light in air using an all-dielectric structure*, Journal of Lightwave Technology **17**(11), 1999, pp. 2039–2041.

[3] HARRINGTON J.A., RABII C., GIBSON D., *Transmission properties of hollow glass waveguides for the delivery of CO_2 surgical laser power*, IEEE Journal of Selected Topics in Quantum Electronics **5**(4), 1999, pp. 948–953.

[4] CHOI S., OH K., SHIN W., RYU U.C., *Low loss mode converter based on adiabatically tapered hollow optical fibre*, Electronics Letters **37**(13), 2001, pp. 823–825.

[5] BIRKS T.A., KNIGHT J.C., RUSSELL P.S.J., *Endlessly single-mode photonic crystal fibre*, Optics Letters **22**(13), 1997, pp. 961–963.

[6] RANKA J.K., WINDELER R.S., STENTZ A.J., *Optical properties of high-delta air–silica microstructure optical fibers*, Optics Letters **25**(11), 2000, pp. 796–798.

[7] EGGLETON B.J., KERBAGE C., WESTBROOK P.S., WINDELER R.S., HALE A., *Microstructured optical fiber devices*, Optics Express **9**(13), 2001, pp. 698–713.

[8] PETROPOULOS P., MONRO T.M., BELARDI W., FURUSAWA K., LEE J.H., RICHARDSON D.J., *2R-regenerative all-optical switch based on a highly nonlinear holey fiber*, Optics Letters **26**(16), 2001, pp. 1233–1235.

[9] FUOCHI M., HAYES J.R., FURUSAWA K., BELARDI W., BAGGETT J.C., MONRO T.M., RICHARDSON D.J., *Polarization mode dispersion reduction in spun large mode area silica holey fibres*, Optics Express **12**(9), 2004, pp. 1972–1977.

[10] CHAUDHURI P.R., LU C., XIAOYAN W., *Scalar model and exact vectorial description for the design analysis of hollow optical fiber components*, Optics Communications **228**(4–6), 2003, pp. 285–293.

[11] JIANPING YIN, YIFU ZHU, *LP_{01}-mode output beam from a micro-sized hollow optical fiber: a simple theoretical model and its applications in atom optics*, Journal of Applied Physics **85**(5), 1999, pp. 2473– 2481.

[12] KEATON G.L., ARBORE M.A., KANE T.J., *Optical wavelength filtering apparatus with depressed--index claddings*, U.S. Patent **6**(563), 2003, pp. 980–995.

[13] ITO H., SAKAKI K., NAKATA T., JHE W., OHTSU M., *Optical potential for atom guidance in a cylindrical-core hollow fiber*, Optics Communications **115**(1), 1995, pp. 57–64.

[14] BARNARD C., MYSLINSKI P., CHROSTOWSKI J., KAVEHRAD M., *Analytical model for rare-earth-doped fiber amplifiers and lasers*, IEEE Journal of Quantum Electronics **30**(8), 1994, pp. 1817–1830.

[15] DIGONNET M.J.F., *Closed-form expressions for the gain in three- and four-level laser fibers*, IEEE Journal of Quantum Electronics **26**(10), 1990, pp. 1788–1796.

[16] ARTIGLIA M., COPPA G., DI VITA P., POTENZA M., SHARMA A., *Mode field diameter measurements in single-mode optical fibers*, Journal of Lightwave Technology **7**(8), 1989, pp. 1139–1152.

[17] SAKAI J., KIMURA T., *Bending loss of propagation modes in arbitrary-index profile optical fibers*, Applied Optics **17**(10), 1978, pp. 1499–1506.

[18] SELVAS R., SAHU J.K., FU L.B., JANG J.N., NILSSON J., GRUDININ A.B., YLÄ-JARKKO K.H., ALAM S.A., TURNER P.W., MOORE J., *High-power, low-noise, Yb-doped, cladding-pumped, three-level fiber sources at 980 nm*, Optics Letters **28**(13), 2003, pp. 1093–1095.

[19] MARCUSE D., *Curvature loss formula for optical fibres*, Journal of the Optical Society of America **66**(3), 1976, pp. 216–220.

[20] COHEN L.G., MARCUSE D., MAMMEL W.L., *Radiating leaky-mode losses in single-mode lightguides with depressed-index claddings*, IEEE Journal of Quantum Electronics **18**(10), 1982, pp. 1467–1472.

Received February 5, 2015
in revised form April 7, 2015